

# Injectable 3D Hydrogel Scaffold with Tailorable Porosity Post-Implantation

Aswan Al-Abboodi, Jing Fu, Pauline M. Doran, Timothy T. Y. Tan,\* and Peggy P. Y. Chan\*

Since rates of tissue growth vary significantly between tissue types, and also between individuals due to differences in age, dietary intake, and lifestyle-related factors, engineering a scaffold system that is appropriate for personalized tissue engineering remains a significant challenge. In this study, a gelatin-hydroxyphenylpropionic acid/carboxymethylcellulose-tyramine (Gtn-HPA/CMC-Tyr) porous hydrogel system that allows the pore structure of scaffolds to be altered *in vivo* after implantation is developed. Cross-linking of Gtn-HPA/CMC-Tyr hydrogels via horseradish peroxidase oxidative coupling is examined both *in vitro* and *in vivo*. Post-implantation, further alteration of the hydrogel structure is achieved by injecting cellulase enzyme to digest the CMC component of the scaffold; this treatment yields a structure with larger pores and higher porosity than hydrogels without cellulase injection. Using this approach, the pore sizes of scaffolds are altered *in vivo* from 32–87  $\mu\text{m}$  to 74–181  $\mu\text{m}$  in a user-controlled manner. The hydrogel is biocompatible to COS-7 cells and has mechanical properties similar to those of soft tissues. The new hydrogel system developed in this work provides clinicians with the ability to tailor the structure of scaffolds post-implantation depending on the growth rate of a tissue or an individual's recovery rate, and could thus be ideal for personalized tissue engineering.

## 1. Introduction

Porosity, pore size, and pore interconnectivity are critical parameters determining the performance of scaffolds in tissue engineering. Pore size affects cell attachment, migration, morphology, and proliferation; porosity and pore structure also have a strong influence on the mechanical properties of the matrix, the supply of nutrients and oxygen, and the removal of waste products.<sup>[1–3]</sup> Different cells and tissues have been shown to require scaffolds of different pore size for maximum tissue growth and development: reports of the optimal average pore size range from as small as 5  $\mu\text{m}$  for neovascularization to 400–500  $\mu\text{m}$  for bone and cartilage regeneration.<sup>[2,4]</sup> In general, relatively small pores are considered advantageous initially to maximize cell attachment and interactivity,<sup>[1]</sup> while highly porous materials provide less diffusional resistance for nutrient and gas exchange.<sup>[4–6]</sup> As porous scaffolds become increasingly occluded due to tissue deposition and develop-

ment, the ability to increase the pore size and porosity *in situ* during cell culture offers significant advantages for improving nutrient, growth factor, and oxygen penetration into the matrix for faster and better tissue growth.

The methods commonly used to fabricate porous scaffolds, such as application of porogens,<sup>[7]</sup> fiber meshes, particulate leaching, gas foaming, electrospinning, freeze-drying, and photo-patterning,<sup>[8]</sup> typically do not allow the porosity or pore size to be tuned once the scaffold is created. *In situ* degradation by hydrolysis or oxidation reactions (through enzyme and cellular activity) to yield lower-molecular-weight compounds may alter the scaffold porosity; however, degradation rates are difficult to control as they depend not only on the composition and cross-link density of the scaffold<sup>[3]</sup> but also on the prevailing physical, chemical, and biological conditions. In particular, once pre-formed porous scaffolds are implanted *in vivo*, very little or no further control can be exerted on the scaffold structure. In this situation, the use of scaffolds that do not degrade fast enough results in restricted cell migration and proliferation and nutrient and oxygen limitations within the developing tissue. On the other hand, a scaffold that degrades too fast can compromise the mechanical and structural integrity of the implant before the tissue is sufficiently well developed. In both cases, tissue regeneration is inhibited due to a mismatch

A. Al-Abboodi  
Department of Chemical Engineering  
Monash University  
Clayton 3800, Australia  
Dr. J. Fu  
Department of Mechanical & Aerospace Engineering  
Monash University  
Clayton 3800, Australia  
Prof. P. M. Doran  
Faculty of Life & Social Sciences  
Swinburne University of Technology  
Hawthorn 3122, Australia  
Prof. T. T. Y. Tan  
School of Chemical & Biomedical Engineering  
Nanyang Technological University  
637459, Singapore  
E-mail: tytan@ntu.edu.sg  
Dr. P. P. Y. Chan  
MicroNanoPhysics Research Laboratory  
School of Applied Science  
RMIT University  
3000, Australia, Melbourne Centre for Nanofabrication  
Australian National Fabrication Facility  
Clayton 3168 Australia  
E-mail: peggy.chan@rmit.edu.au



DOI: 10.1002/adhm.201300303

between the rates of tissue growth and scaffold degeneration. Because different tissues have widely different regeneration rates,<sup>[3]</sup> and as cell and tissue growth can also vary significantly between individuals due to differences in age, dietary intake, and lifestyle-related factors,<sup>[9–11]</sup> engineering a scaffold system that is most appropriate for different tissues and individuals is very challenging.

In this work, we address the problem of pore size and porosity control in scaffolds by developing a hydrogel system that allows the pore structure to be altered in vivo after implantation. This new approach gives users the ability to tailor the scaffold architecture to match the specific growth rate of a tissue or an individual's recovery rate. This was accomplished by synthesizing two polymers: phenol containing gelatin, namely gelatin-hydroxyphenylpropionic acid (Gtn-HPA), as the hydrogel backbone, and phenol containing cellulose, namely carboxymethylcellulose-tyramine (CMC-Tyr), to induce phase separation as well as acting as a sacrificing polymer. The two polymers were cross-linked via horseradish peroxidase (HRP)-mediated oxidation to yield a porous hydrogel. The Gtn-HPA conjugate was first developed by Kurisawa and co-workers as a precursor to form injectable hydrogel scaffolds for tissue engineering: Gtn-HPA hydrogel was cross-linked via oxidative coupling of phenol moieties catalyzed by HRP and dilute hydrogen peroxide ( $\text{H}_2\text{O}_2$ ).<sup>[12]</sup> The backbone of this hydrogel contains gelatin that can be degraded by a number of proteases,<sup>[13]</sup> thereby rendering the Gtn-HPA hydrogel biodegradable.

Injectable hydrogels can also be produced by other methods, for example, physical cross-linking by ionic interactions or sol-gel transition, or chemical cross-linking by Michael-type addition reaction, disulfide bond formation or aldehydes. However, the gelation time of these hydrogels is usually controlled by varying the cross-linker or gel precursor concentration, which inevitably changes the mechanical strength of the resulting matrix.<sup>[12]</sup> In contrast, peroxidase-catalyzed cross-linking gives rise to hydrogels with mechanical strength and gelation rates that are independently tunable.<sup>[12]</sup> The gelation time (ranging from 1 s to 20 min) of Gtn-HPA hydrogel can be tuned solely by the HRP concentration, while the mechanical strength can be tuned solely by the  $\text{H}_2\text{O}_2$  concentration.<sup>[14]</sup> Peroxidase-catalyzed cross-linking is an attractive strategy as the enzymatic coupling can be carried out at room temperature and in an aqueous environment without the use of organic solvents or toxic crosslinkers: in situ cell immobilization can therefore take place by simply mixing the cells with the gel precursor. For example, continuous production of cell-seeded Gtn-HPA hydrogel fibers has been demonstrated using a spinning system and triple-orifice extruder.<sup>[15,16]</sup>

Gtn-HPA hydrogels have been demonstrated as a promising scaffold material for tissue engineering. For instance, neurogenesis and myogenesis of human mesenchymal stem cells (hMSCs) can be controlled by simply tuning the Gtn-HPA hydrogel stiffness without the use of additional biochemical signals.<sup>[14,17]</sup> Peroxidase-mediated coupling has also been employed to cross-link various other phenol-containing polymers and is well known to yield in situ hydrogels that are biocompatible with encapsulated cells.<sup>[15,18–20]</sup> For example, Kurisawa and co-workers<sup>[21,22]</sup> have demonstrated that hydrogels

produced using peroxidase-mediated oxidation support neural and mesenchymal stem cell viability at levels greater than 90%. Peroxidase-mediated oxidation has also been shown to produce in situ hydrogels that are biocompatible in vivo.<sup>[23–25]</sup> However, such injectable hydrogels do not contain any micropores or macropores (see Figure S1, Supporting Information); in addition, the porosity or pore size of the gel cannot be tuned once the hydrogel is created. Here, we describe a new method to increase the pore size and porosity of tissue engineering scaffolds post-implantation using cellulase injection to digest the sacrificing polymer, cellulose, in hydrogels. In addition, as the hydrogel is cross-linked by HRP, it is injectable and suitable for applications in laparoscopic surgery.

## 2. Materials and Methods

### 2.1. Preparation of Gtn-HPA/CMC-Tyr Hydrogel

CMC-Tyr conjugates were synthesized using a general carbodiimide/active ester-mediated coupling reaction in distilled water. Briefly, CMC (5 g) and Tyr (0.864 g) were dissolved in milliQ water (250 mL). To this solution, N-hydroxysuccinimide (NHS) (0.573 g) and 1-ethyl-3-(3-dimethylaminopropyl)-carbodiimide hydrochloride (EDC) (0.955 g) were added. The mixture was stirred overnight at room temperature and pH 4.7. The products were dialyzed against  $100 \times 10^{-3}$  M NaCl, 25% ethanol, and water in sequence for 2 d each, and then lyophilized. Conjugation of tyramine to CMC was confirmed by  $^1\text{H}$  NMR ( $\text{D}_2\text{O}$ ); chemical shifts were detected at  $\delta$  6.8 and 7.2 indicated the presence of aromatic protons of tyramine on CMC. Gtn-HPA conjugates were prepared according to Wang et al.<sup>[17]</sup> To synthesize fluorescently labeled Gtn-HPA, the  $-\text{COOH}$  group of Gtn-HPA conjugates (10 g) were activated using NHS/EDC at pH 4.8 for 15 min. Fluoresceinamine isomer I (Sigma) dissolved in methanol ( $0.23 \times 10^{-6}$  M) was added dropwise to the Gtn-HPA conjugates while stirring and the reaction was allowed to proceed overnight in the dark. The products were purified by dialysis and then lyophilized.

Lyophilized Gtn-HPA and lyophilized CMC-Tyr were each dissolved in separate phosphate buffered saline (PBS) solutions at a concentration of 5% (w/v). Hydrogel precursor solution was prepared by mixing the Gtn-HPA and CMC-Tyr solutions using a 80:20 weight ratio, respectively. Cross-linking was initiated by adding HRP to give three different final concentrations (3.9, 7.7, and 15.5 unit  $\text{L}^{-1}$ ) and diluted  $\text{H}_2\text{O}_2$  to give a final concentration of  $49.8 \times 10^{-6}$  M.

### 2.2. Adjusting the Pore Size In Situ

Cellulase from *Trichoderma longibrachiatum* (Sigma;  $\geq 1.0$  unit  $\text{mg}^{-1}$ ) was dissolved in PBS at a concentration of 0.1  $\text{mg mL}^{-1}$  and sterilized by syringe filtration. Hydrogel precursor solution with added HRP and  $\text{H}_2\text{O}_2$  was injected between two parallel glass plates clamped together with 1 mm spacing. The cross-linking reaction was allowed to proceed at 37 °C. Round hydrogel disks of diameter 1.5 cm were then cut out using a circular mold. The hydrogel disks were immersed in PBS at

37 °C for 24 h to reach swelling equilibrium. The swollen hydrogels were then immersed in cellulase solution (0.1 mg mL<sup>-1</sup> in PBS). Spent solution was replaced by cellulase solution daily. The time-course of hydrogel digestion was examined over a period of up to 9 d by measuring the dry weight of residual hydrogel after oven drying at 50–60 °C to constant weight. Disks of Gtn-HPA hydrogel without cellulose content were used as controls. The pore sizes and porosities of lyophilized hydrogels were determined using a mercury porosimeter (Autopore II 9220; Micromeritics) and are reported as mean ± standard deviation. The Z-test ( $n > 30$ ) was used to compare the results statistically before and after cellulase digestion.

### 2.3. Swelling Ratio Measurement

The swelling ratio of hydrogel was evaluated using a classical gravimetric method. Hydrogel disks prepared using  $49.8 \times 10^{-6}$  M of H<sub>2</sub>O<sub>2</sub> and three different HRP concentrations (3.9, 7.7, and 15.5 unit L<sup>-1</sup>) were swollen in PBS at 37 °C for 2 d to reach swelling equilibrium. To obtain cellulase-digested hydrogel disks, these hydrogels were immersed in cellulase solution (0.1 mg mL<sup>-1</sup> in PBS) at 37 °C for 24 h. Spent solution was replaced by 1 mL of fresh cellulase solution daily for a period of 3 d. The cellulase-treated hydrogels were rinsed with MilliQ water for 2 d to remove residual cellulase. The surface of the swollen disks with or without cellulase treatment was gently blotted with Kimwipe and weighed immediately to obtain the swollen weight. The swollen disks were then lyophilized and the dry weight of the lyophilized disks was measured. The swelling ratio was calculated according to:

$$\text{Swelling ratio} = \frac{W_s - W_d}{W_s} \times 100\% \quad (1)$$

where  $W_s$  and  $W_d$  are the weights of swollen and dry hydrogels, respectively.

### 2.4. Measurement of Rheological and Mechanical Properties

Measurements of gelation time, loss modulus, and storage modulus of hydrogel prior to cellulase digestion were performed according to Wang et al.<sup>[14]</sup> To assess the mechanical properties of hydrogel after cellulase digestion, Gtn-HPA/CMC-Tyr hydrogel precursor solution prepared using three different concentrations of HRP (3.9, 7.7, and 15.5 unit L<sup>-1</sup>) and a fixed concentration of H<sub>2</sub>O<sub>2</sub> ( $49.8 \times 10^{-6}$  M) was injected between two parallel glass plates clamped together with 1 mm spacing. After cross-linking, round hydrogel disks of diameter 1.5 cm were cut out using a circular mold. The hydrogel disks were immersed in 1 mL of cellulase solution (0.1 mg mL<sup>-1</sup> in PBS) at 37 °C for 24 h. Spent solution was replaced by 1 mL of fresh cellulase solution daily for a period of 3 d. The storage modulus of the swollen hydrogels was measured using a Haake MARS (Modular Advanced Rheometer System, Germany) at 37 °C in the dynamic oscillatory mode with a constant deformation of 0.5% and a frequency of 0.5 Hz.

### 2.5. Cytocompatibility and Cell Proliferation Assays

The cytocompatibility of the hydrogel was evaluated using COS-7 cells. Lyophilized Gtn-HPA and CMC-Tyr were dissolved in 500 µL of Dulbecco's Modified Eagle Medium (DMEM) supplemented with 10% (v/v) fetal bovine serum (FBS),  $2 \times 10^{-3}$  M L-glutamine, and 50 units mL<sup>-1</sup> penicillin–streptomycin, and sterilized immediately by syringe filtration through a 0.2-µm filter. African green monkey kidney (COS-7) cells at a density of  $1 \times 10^4$  cells mL<sup>-1</sup> were mixed with the sterilized solution prior to cross-linking. Cross-linking was initiated by adding diluted H<sub>2</sub>O<sub>2</sub> and different concentrations of HRP and allowed to proceed at 37 °C in a humidified 5% CO<sub>2</sub> incubator. To adjust the pore size in situ, the hydrogel was incubated in medium containing cellulase (0.1 mg mL<sup>-1</sup>) at 37 °C; spent medium was replaced by fresh cellulase-containing medium daily. COS-7 cells were harvested at different time points over a period of 7 d by digesting the hydrogel using trypsin and cellulase. Cell number was determined by quantifying the DNA content using a Quant-iT PicoGreen dsDNA assay kit (Invitrogen) according to the manufacturer's protocol. The total DNA content in each hydrogel sample was determined by measuring the fluorescence using a SpectraMax M2 microplate reader (Molecular Devices) at an excitation wavelength of 480 nm and an emission wavelength of 520 nm. The number of cells in each sample was calculated by correlating the total DNA content with a known number of COS-7 cells. These experiments were performed using triplicate gels for each time point and HRP concentration.

### 2.6. Subcutaneous Formation of Hydrogel In Vivo

The animal studies were approved by the Institutional Animal Care and Use Committee (IACUC0092), Nanyang Technological University, and all experiments were carried out in compliance with the necessary regulations. All animals were maintained in pathogen-free conditions. Two milliliters of hydrogel precursor solution containing CMC-Tyr, fluorescently labeled Gtn-HPA,  $49.8 \times 10^{-6}$  M H<sub>2</sub>O<sub>2</sub>, and different concentrations of HRP (3.9, 7.7, and 15.5 unit L<sup>-1</sup>) were administered by dorsal subcutaneous injection to female Lewis rats (6–8 weeks old). Six rats were used for each HRP concentration. The hydrogels were allowed to gelify in situ. To adjust the pore size of the hydrogels, 0.3 mL of 0.1 mg mL<sup>-1</sup> cellulase in PBS was injected into the animals at the same position as the scaffold 2 h after the initial injection of hydrogel. Triplicate rats were injected with cellulase for each HRP concentration, leaving triplicate control animals for each HRP concentration without cellulase treatment. Six hours after the initial hydrogel injection, the animals were anesthetized and then sacrificed by intra-cardiac injection of an overdose of pentobarbital. The skin was incised to expose the hydrogel scaffolds, which were excised and fixed in 4% formalin. In order to investigate the effect of introducing cellulase at later time points, another set of in vivo experiments was carried out using the above procedure, except that three doses of cellulase (0.3 mL of 0.1 mg mL<sup>-1</sup> cellulase in PBS, 24 h between injections) were injected into the animal starting from day 4 after the initial injection of hydrogel. The animals were

sacrificed 7 d after the initial hydrogel injection. The cross-sectional morphologies of the harvested hydrated hydrogels were visualized using LSCM. Samples were also lyophilized for SEM analysis. Pore sizes were measured from the LSCM images and are reported as mean  $\pm$  standard deviation ( $n = 25\text{--}50$ ). One-way analysis of variance (ANOVA) was used to compare multiple groups of data; the Student's *t*-test was used to compare two groups of data.

### 3. Results and Discussion

#### 3.1. Hydrogel Formation

The scaffold fabrication process described in this study is simple and biocompatible. Two phenol-containing polymers, gelatin-hydroxyphenylpropionic acid (Gtn-HPA)<sup>[17]</sup> as the hydrogel scaffold backbone, and carboxymethylcellulose-tyramine (CMC-Tyr) (Figure 1a) as a sacrificing polymer were synthesized. The Gtn-HPA component contains Arg-Gly-Asp (RGD) peptides that act as cell adhesive ligands. The two polymer conjugates were dissolved together in PBS and appear as a clear solution; HRP and diluted hydrogen peroxide ( $\text{H}_2\text{O}_2$ ) were then added to the solution. At this stage, for in vivo applications, the hydrogel may be injected to fill any irregularly shape defect. The polymer conjugates were allowed to cross-link to form a polymer network via peroxidase-catalyzed oxidative coupling of the HPA and Tyr moieties (Figure 1b). It is well known that cross-linking occurs at the C-C and C-O position of phenols;<sup>[26]</sup> this reaction proceeds rapidly in aqueous solution at room temperature<sup>[27]</sup> so that living cells can be incorporated during cross-linking for in situ immobilization. Figure 1c summarizes the procedures involved in preparing the porous hydrogel. A porous polymer network or hydrogel scaffold was obtained after cross-linking, with pore formation driven by phase separation between Gtn-HPA and CMC-Tyr. The former biopolymer contains gelatin that is known to contain both hydrophilic and hydrophobic peptides,<sup>[13]</sup> while the latter biopolymer is rich in carboxylic acid residues and thus more hydrophilic than Gtn-HPA. The resulting hydrogel appears optically opaque upon cross-linking; this opaque appearance is a typical characteristic of hydrogels formed via phase separation.<sup>[28–30]</sup> The mechanisms of phase separation relevant to this system are discussed in more detail in the literature.<sup>[31–33]</sup>

To alter the hydrogel structure post-implantation, diluted cellulase enzyme ( $0.1 \text{ mg mL}^{-1}$  in PBS) was injected into the hydrogel scaffold to digest the sacrificing polymer, CMC, to glucose or low-molecular-weight CMC via hydrolysis of the glucosidic linkages in CMC (Figure 2). These low-molecular-weight molecules are able to diffuse out of the porous hydrogel network to yield a material with higher porosity and larger pore size compared with hydrogel before cellulase treatment. The cellulase used was derived from *Trichoderma longibrachiatum*, has a long history of safe use in the food industry, has been affirmed by the US Food and Drug Administration (FDA) to be Generally Recognized As Safe (GRAS).<sup>[34]</sup> Since the rate and extent of cellulase digestion can be controlled by varying the amount and frequency of cellulase injection, it is possible for clinicians using this system to alter the hydrogel pore structure in a controllable manner post-implantation.

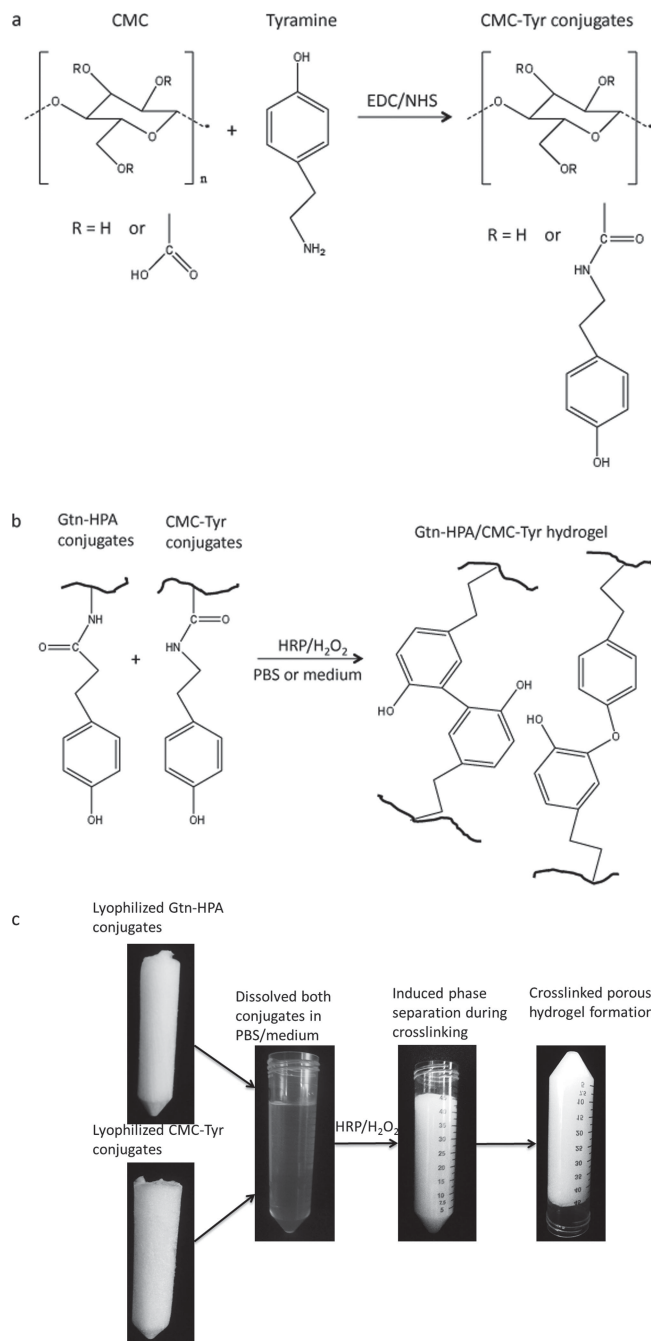


**Figure 1.** a) Synthesis scheme of CMC-Tyr conjugates; b) CMC-Tyr and Gtn-HPA conjugates were cross-linked by peroxidase-catalyzed oxidation. c) Preparation of 5% Gtn-HPA/CMC-Tyr hydrogel. Lyophilized Gtn-HPA and lyophilized CMC-Tyr were first dissolved to form a homogeneous solution at room temperature. HRP and diluted  $\text{H}_2\text{O}_2$  were then added to the solution to cross-link Gtn-HPA and CMC-Tyr to form an opaque gel at room temperature.

#### 3.2. In Vitro Pore Size and Porosity

The hydrogels were further characterized using mercury porosimetry to measure the in vitro pore size and porosity of the scaffolds with and without cellulase digestion. These properties

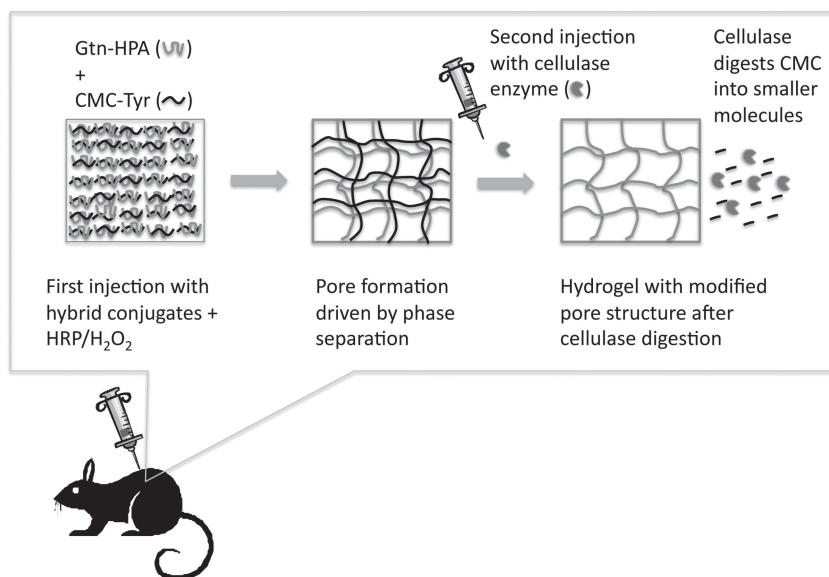


**Figure 2.** Schematic representation of the formation of injectable hydrogel by HRP-catalyzed oxidation with in situ pore size control using cellulase digestion.

varied depending on the HRP concentration used (Table 1): hydrogels produced using the highest HRP concentration (15.5 unit L<sup>-1</sup>) exhibited the smallest pore size and porosity, while hydrogels produced using the lowest HRP concentration (3.9 unit L<sup>-1</sup>) exhibited the largest pore size and porosity. The results demonstrate that HRP concentration is a critical factor affecting the pore structure of the hydrogel, most likely through its effect on phase separation during hydrogel formation. Despite both proteins and polysaccharides being soluble in an aqueous solution, it has been reported that these macromolecules normally have limited compatibility at the molecular level, so that each macromolecule tends to be surrounded by its own species in mixed solution, thereby causing the mixture to separate into different liquid phases.<sup>[35]</sup> The mixture of Gtn-HPA and CMC-Tyr is initially homogeneous and miscible; however, upon cross-linking, further phase separation occurs as the fraction of molecules with high molecular weight increases, causing the morphology of the mixture to separate into discrete domains. Reducing the concentration of HRP and therefore the rate of cross-linking probably allows time for these discrete domains to increase in size and undergo a phenomenon

known as spinodal decomposition<sup>[31]</sup> so that a porous matrix with relatively large voids is formed.

Cellulase treatment was performed in vitro to alter the hydrogel pore structure post-fabrication. Figure 3 shows representative SEM images of lyophilized hydrogel with or without cellulase treatment. These images show that pore sizes in the hydrogel decreased as the concentration of HRP decreased. It can also be observed that the pore sizes increased after cellulase treatment. These observations will be discussed in detail in later sections. Cellulase digestion for 24 h resulted in an increase in mean pore size of 31% ( $p < 0.0001$ ) and 61% ( $p = 0.003$ ) for hydrogels produced using 3.9 and 15.5 unit L<sup>-1</sup> HRP, respectively (Table 1); the 8% increase in pore size measured using 7.7 unit L<sup>-1</sup> HRP was not statistically significant ( $p = 0.376$ ). Hydrogel porosity was also enhanced after cellulase treatment: the mean porosity increased by 11% ( $p = 0.010$ ) and 48% ( $p < 0.0001$ ) after cellulase digestion of hydrogels produced using 7.7 and 15.5 unit L<sup>-1</sup> HRP, respectively; the measured increase in porosity for the 3.9 unit L<sup>-1</sup> HRP samples was not statistically significant ( $p = 0.426$ ).

### 3.3. Weight Loss Induced by Cellulase Digestion

To quantify the extent of cellulase digestion, Gtn-HPA/CMC-Tyr hydrogels produced using different HRP concentrations were treated with cellulase; hydrogels composed of pure Gtn-HPA only were used as controls. Whereas the Gtn-HPA/CMC-Tyr hydrogels were digested as indicated by weight loss measurements, the Gtn-HPA matrix remained unaffected (Figure 4). This result confirms the specificity of cellulase for digestion of cellulose in the CMC polymer, thus allowing Gtn-HPA in the Gtn-HPA/CMC-Tyr hydrogels to function as the cell adhesive structure that remains intact during cellulase treatment. The substrate specificity of cellulase also means that newly formed extracellular matrix (ECM) secreted by cells in the hydrogel is unlikely to be affected by cellulase treatment. In general, the rate of digestion observed for the Gtn-HPA/CMC-Tyr hydrogels

**Table 1.** Mean pore size and porosity of in vitro Gtn-HPA/CMC-Tyr hydrogels with and without cellulase digestion. For cellulase digestion, hydrogel disks were digested by cellulase solution (0.1 mg mL<sup>-1</sup> in PBS) for a period of 3 d; spent solution was replaced with fresh cellulase solution daily. Results are shown as mean  $\pm$  standard deviation.

HRP concentration [unit L <sup>-1</sup> ]	Mean pore size before cellulase digestion [ $\mu$ m]	Mean pore size after cellulase digestion [ $\mu$ m]	Increase in pore size after cellulase digestion [%]	Mean porosity before cellulase digestion [%]	Mean porosity after cellulase digestion [%]	Increase in porosity after cellulase digestion [%]
3.9	52 $\pm$ 8.9	68 $\pm$ 3.0	31 <sup>a)</sup>	86 $\pm$ 2.2	88 $\pm$ 4.1	2
7.7	38 $\pm$ 6.5	41 $\pm$ 5.0	8	64 $\pm$ 4.1	71 $\pm$ 3.3	11 <sup>a)</sup>
15.5	18 $\pm$ 6.4	29 $\pm$ 7.3	61 <sup>a)</sup>	31 $\pm$ 5.5	46 $\pm$ 3.2	48 <sup>a)</sup>

<sup>a)</sup>At the same HRP concentration, the difference between hydrogel before cellulase digestion and hydrogel after cellulase digestion is statistically significant at  $p < 0.01$ .

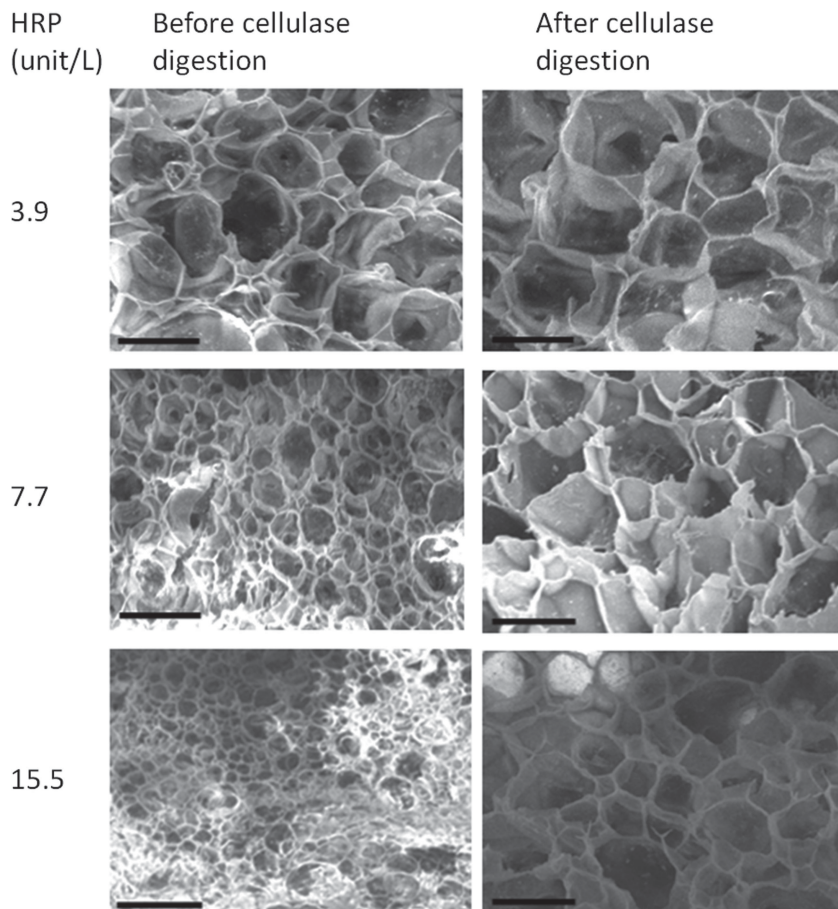


**Figure 3.** Typical cross-sectional SEM images of lyophilized in vitro hydrogels prepared using 3.9, 7.7, and 15.5 unit L<sup>-1</sup> HRP. For cellulase digestion, hydrogel disks were digested in cellulase solution (0.1 mg mL<sup>-1</sup> in PBS) for a period of 3 d, followed by rinsing and lyophilization. Scale bars represent 50 μm.

increased as the HRP concentration used to produce the scaffolds decreased (Figure 4). This is consistent with the larger pore sizes and higher porosities observed at lower HRP levels

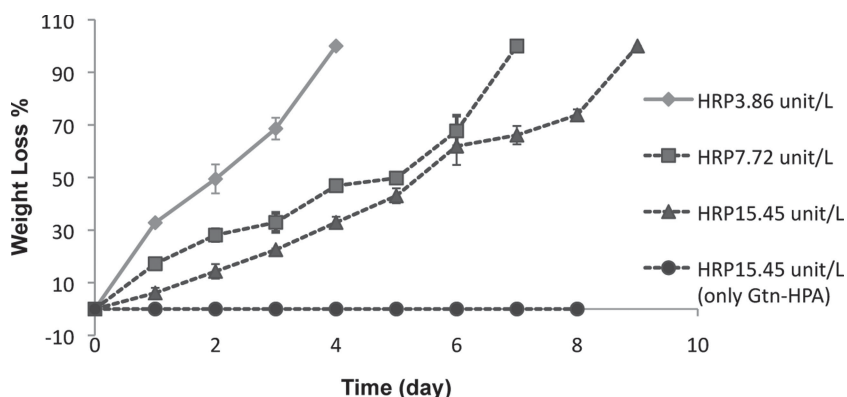


**Figure 4.** Scaffold weight loss during enzymatic digestion of Gtn-HPA/CMC-Tyr and Gtn-HPA hydrogels in the presence of 0.1 mg mL<sup>-1</sup> cellulase at 37 °C. The hydrogels were prepared using different concentrations of HRP. The error bars represent standard deviation ( $n = 3$ ).

(Table 1), which would facilitate more rapid penetration of cellulase into the hydrogel structure. These experiments demonstrate that it is possible to quantify cellulase digestion of the scaffolds and to generate data useful for tailoring the pore structure of scaffolds post-implantation to match the growth rate of specific tissues.

### 3.4. Swelling Ratio

Figure 5a,b shows the swelling ratios of hydrogel before and after cellulase digestion, respectively. Swelling ratio represents the amount of water that can be absorbed by the hydrogel; this is an important property as high swelling ratios can facilitate diffusion of nutrients, oxygen, and metabolites.<sup>[28]</sup> It is well known that the presence of open pores in hydrogels allows water to be absorbed by convection.<sup>[36]</sup> Before cellulase digestion, the hydrogels prepared using three different HRP concentrations exhibited high swelling ratios reflecting the presence of porous structures. The swelling ratio was found to increase with decreasing HRP concentration: hydrogels prepared using lower HRP concentration (i.e., 3.9 unit mL<sup>-1</sup>) contained larger pores, thus facilitating better water infiltration into the porous network. After cellulase digestion, the swelling ratios of the resulting hydrogels were enhanced, as the pores were opened up by cellulase digestion, thus allowing more water infiltration. After cellulase digestion, the swelling ratios continued to increase with decreasing concentration of HRP, consistent with the increase in pore size and porosity of the hydrogels with decreasing HRP concentration.

### 3.5. Rheology and Mechanical Properties of Hydrogels

The physical, mechanical, and biocompatibility properties of the hydrogel were first characterized in vitro. Hydrogels were prepared using the same polymer composition and H<sub>2</sub>O<sub>2</sub> concentration but with different concentrations of HRP enzyme for catalyzing the cross-linking reaction. The formation of Gtn-HPA/CMC-Tyr hydrogels was investigated using oscillatory rheometry techniques. The typical evolution with cross-linking time of the storage modulus ( $G'$ ) and loss modulus ( $G''$ ) of hydrogels is shown in the Supporting Information (Figure S2a–c). The crossover of the two moduli is defines as

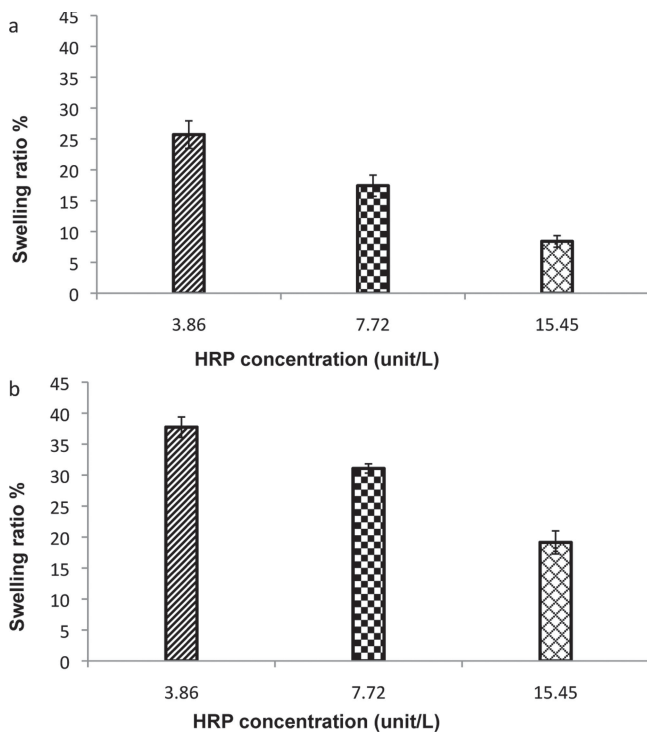


**Figure 5.** Swelling ratios of a) Gtn-HPA/CMC-Tyr hydrogels prepared using 3.9, 7.7, and 15.5 unit L<sup>-1</sup> HRP without cellulase treatment, and b) cellulase-digested Gtn-HPA/CMC-Tyr hydrogels prepared using 3.9, 7.7, and 15.5 unit L<sup>-1</sup> HRP. The error bars represent standard deviation ( $n = 3$ ).

the gel point at which the viscoelastic liquid transforms into a viscoelastic solid, and the time required to reach the gel point is defined as the gelation time. The gelation rate was found to increase with increasing HRP concentration: gelation times of  $\approx 597$ , 330, and 110 s were obtained for hydrogels prepared using HRP concentrations of 3.9, 7.7, and 15.5 unit L<sup>-1</sup>, respectively. However, the corresponding values of  $G'$  were similar at 3741, 3898, and 3933 Pa, respectively. The control group prepared with 0 unit L<sup>-1</sup> of HRP did not gelify. As with other HRP-mediated cross-linked hydrogel systems,<sup>[14,23]</sup> the mechanical properties of the Gtn-HPA/CMC-Tyr hydrogel were independent of gelation rate<sup>[14]</sup> and similar to those of soft tissues and organs.<sup>[37]</sup>

Pore size and porosity have little effect on the storage modulus of Gtn-HPA/CMC-Tyr hydrogels, as the mechanical properties of the hydrogels were measured using swollen samples, in which the hydrostatic effect of water entrapped in the scaffold pores reduces the deformability of the scaffold<sup>[38]</sup> has also reported that the storage modulus was less dependent on pore size and porosity in starch/poly(L-lactic) acid scaffolds that were immersed under physiological conditions. In contrast, the storage modulus was dependent on pore size and porosity for samples measured in a dry state. Since the Gtn-HPA/CMC-Tyr hydrogels in the present study are intended for in vivo applications, it is more appropriate to perform the measurement of mechanical properties using wet samples immersed in physiological simulated solution.

The storage modulus of hydrogels after cellulase digestion was also evaluated. As expected,  $G'$  decreased after cellulase digestion: the values of  $G'$  were 2788, 3041, and 3362 Pa for hydrogels prepared with HRP concentrations of 3.9, 7.7, and 15.5 unit L<sup>-1</sup>, respectively. The values of  $G'$  decreased with decreasing HRP concentration, which is likely due to the larger mass of cellulose lost during enzymatic digestion of hydrogels prepared with lower HRP concentration (Figure 4). A reduction in mechanical strength associated with scaffold degradation is expected in a biodegradable scaffold, and can be beneficial for tissue regeneration, as softer scaffolds allow new tissue to more easily infiltrate the scaffold.

### 3.6. In Vitro Cytocompatibility

To assess the cytocompatibility of the scaffolds, COS-7 cells were immobilized in Gtn-HPA/CMC-Tyr hydrogels in situ prior to cross-linking with HRP/H<sub>2</sub>O<sub>2</sub>. Mixing cells suspended in culture medium with polymer conjugates before cross-linking yields homogeneously seeded scaffolds and overcomes the difficulties associated with introducing cells and achieving uniform cell distributions within already gellified structures. The viability of COS-7 cells remained high after in situ immobilization (see Supporting Information). The number of cells inside the scaffolds was quantified by measuring the DNA content, as DNA is the cellular component that most accurately reflects cell number.<sup>[39]</sup> The DNA content, and thus the number of cells, in the scaffolds increased over the 7-d culture period (Figure 6), indicating that the encapsulated cells were viable and capable of proliferation, and confirming that the Gtn-HPA/CMC-Tyr hydrogel is biocompatible for tissue engineering applications. Cell growth was faster as the HRP concentration used for cross-linking was reduced; hydrogels with larger pores and porosities (produced using lower HRP concentrations; Table 1) provide entrapped cells with better access to nutrients and oxygen and more space for migration and proliferation than scaffolds with restricted pore structure. However, growth of cells in hydrogels without cellulase treatment showed signs of slowing down after about 4 d (Figure 6). In contrast, when the hydrogels were digested with cellulase starting on day 1 of the culture, significant further cell growth occurred after 4 days and the final cell numbers obtained were significantly higher than those achieved under the same conditions without cellulase digestion. For each HRP concentration, the final cell numbers obtained from hydrogels digested by cellulase starting from day 4 were similar to those found after digestion by cellulase starting from day 1 (Figure 6c).

As well as demonstrating the benefits of manipulating the scaffold pore size and porosity post-inoculation, these results show that cellulase treatment has no toxic effects on the cells. The approach to hydrogel fabrication and manipulation developed in this work allows scaffolds with smaller pore sizes and porosities to be used at the beginning of tissue engineering cultures when achieving cell attachment is critical,<sup>[1]</sup> while providing the opportunity to tailor the scaffold and enlarge the pores as required at the desired time to improve cell proliferation, transport of nutrients, and tissue formation.

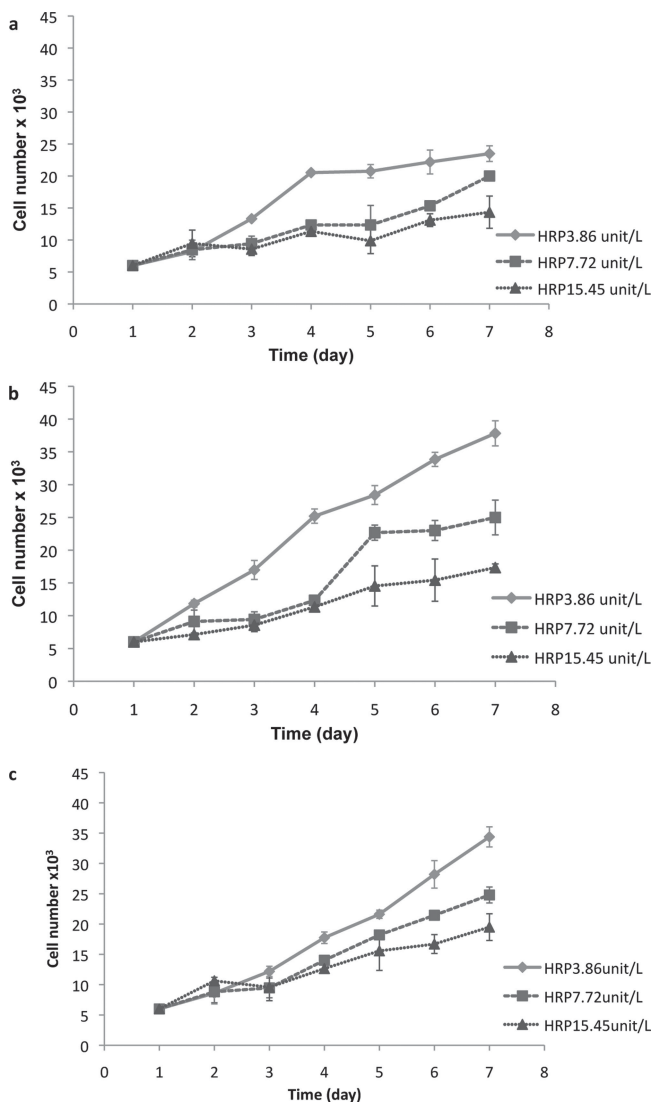


**Figure 6.** Proliferation of COS-7 cells in vitro in a) Gtn-HPA/CMC-Tyr hydrogels without cellulase treatment, b) Gtn-HPA/CMC-Tyr hydrogels with cellulase treatment ( $0.1 \text{ mg mL}^{-1}$  in medium) started from day 1, and c) Gtn-HPA/CMC-Tyr hydrogels with cellulase treatment ( $0.1 \text{ mg mL}^{-1}$  in medium) started from day 4. During cellulase treatment, spent medium was replaced by fresh cellulase solution daily. The error bars represent standard deviation ( $n = 3$ ).

### 3.7. Subcutaneous Formation of Hydrogels

To examine the ability of the Gtn-HPA/CMC-Tyr hydrogels to cross-link in vivo, and to demonstrate the feasibility of tuning hydrogel pore size and porosity post-implantation, Gtn-HPA and CMC-Tyr hydrogel precursors were injected into the dorsal subcutis of female Lewis rats (Figure 7a,b). Fluorescein isothiocyanate (FITC)-labeled Gtn-HPA was used to assist visualization. The gelation time for formation of gelified lumps of size 0.8–1.3 cm within the subcutaneous layer depended on the HRP concentration applied consistent with the in vitro results. Post-gelation, cellulase was injected directly into each lump to alter the pore size and porosity of the hydrogel in vivo

(Figure 7b). Animals with no cellulase treatment were used as the control group (Figure 7a). After the animals were sacrificed, the hydrogel implants were detected easily within the subcutaneous space. No pathological reactions were observed within the implants or the subcutaneous wall.

The microscopic morphologies of the in vivo hydrogel implants in the control groups were investigated. Figure 8a–c shows typical images of cross-sections of the hydrated implants obtained using laser scanning confocal microscopy (LSCM); these implants were composed of CMC-Tyr and FITC-labeled Gtn-HPA without cellulase treatment. Figure 9a–c shows typical cross-sections observed using scanning electron microscopy (SEM) after lyophilization of hydrogel implants harvested 6 h after initial injection of hydrogels without cellulase treatment. The LSCM and SEM images reveal the presence of a homogeneous interconnected macroporous structure in both hydrated and lyophilized hydrogel implants. Such networks of interconnected pores are important for supporting cell proliferation and deposition of ECM during tissue regeneration, and for facilitating exchange of oxygen and nutrients throughout the hydrogel. The LSCM images revealed that as the HRP concentration decreases, thus increasing the gelation time, a coalescence of Gtn-HPA-rich domains can be visualized in the hydrogel. Such morphologies are typically observed in ternary biopolymer systems (consisting of two biopolymers and a solvent) that undergo phase separation by spinodal decomposition.<sup>[31]</sup>

Similar to the in vitro results (Figure 3, Table 1), pore sizes in the in vivo hydrogels varied with the concentration of HRP used for polymer cross-linking: visually in Figures 8a–c, 9a–c, the pores were larger in hydrogels produced using the lowest HRP concentration (Figures 8a, 9a) and smaller in hydrogels produced using the highest HRP concentration (Figures 8c, 9c). As indicated in the LSCM images of the hydrated scaffolds (Figure 8a–c), pore sizes in the in vivo hydrogels were distributed bimodally: many small micropores were located within the polymeric material bridging between larger macropores. The diameter of the larger pores decreased as the concentration of HRP applied for cross-linking was increased ( $p < 0.0001$ ) and were (mean  $\pm$  standard deviation)  $87 \pm 2.1$ ,  $51 \pm 5.2$ , and  $32 \pm 1.3 \mu\text{m}$  for hydrogels prepared using 3.9, 7.7, and 15.5  $\text{unit L}^{-1}$  HRP, respectively. The diameter of the smaller pores also decreased with increasing HRP concentration ( $p < 0.0001$ ) and were  $19 \pm 3.4$ ,  $11 \pm 7.2$ , and  $9 \pm 8.2 \mu\text{m}$  for HRP concentrations 3.9, 7.7, and 15.5  $\text{unit L}^{-1}$ , respectively. Compared to hydrogels harvested 6 h post-implantation, the diameter of both the larger ( $p < 0.0001$ ) and smaller pores ( $p < 0.01$ ) increased in hydrogels harvested 7 d post-implantation (Figures 8g–i, 9g–i), probably due to the presence of in vivo proteases, which may also contribute to in vivo hydrogel degradation.

### 3.8. Adjusting the Pore Size Post-Implantation

Figure 8d–f shows typical LSCM images of cross-sections of hydrated hydrogel implants after in vivo treatment with cellulase 2 h post-implantation. Figure 9d–f shows the corresponding SEM images of cellulase-treated hydrogels after lyophilization. In vivo cellulase digestion resulted in an increase in pore size

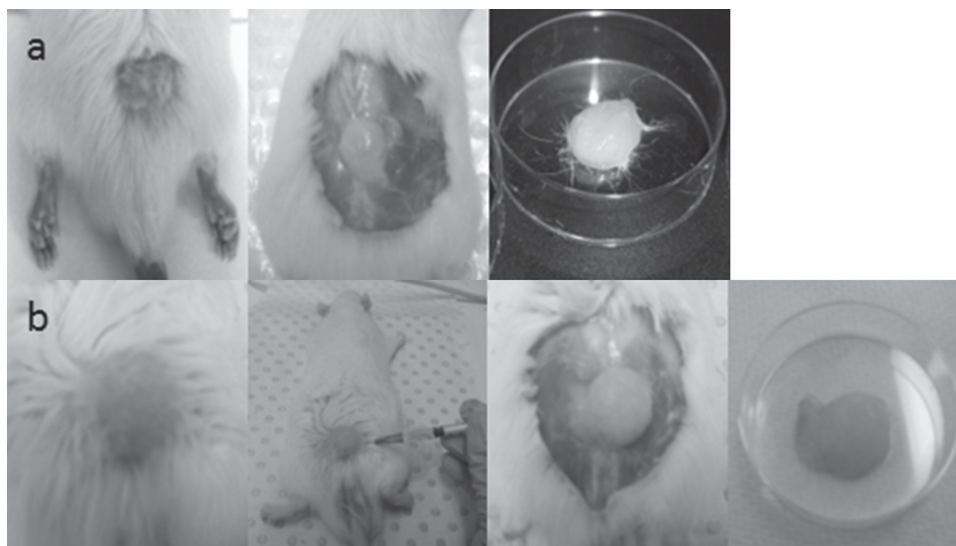


**Figure 7.** a) Female Lewis rats were injected subcutaneously with Gtn-HPA/CMC-Tyr precursor solution, diluted  $\text{H}_2\text{O}_2$  and HRP. In situ gelation of the hydrogel within the subcutaneous layer can be observed. b) After injection with hydrogel solution and cross-linking, rats were also injected with cellulase solution into the hydrogel for digestion of CMC and modification of the scaffold pore size.

and porosity: the cellulase-digested hydrogels have a more open and accessible pore structure compared with untreated samples produced using the same HRP concentration. The homogeneity of the porous networks after cellulase treatment indicates that cellulase penetrated throughout the entire volume of the hydrogel lumps to digest CMC at all locations within the scaffolds. The cellulase-digested hydrogels continued to exhibit a bimodal distribution of pore sizes: micropores were present

within the polymer surrounding much larger macropores (Figure 8d–f). For hydrogels treated with cellulase and harvested after 6 h, the diameters of the larger pores decreased with increasing HRP concentration ( $p < 0.0001$ ) and were  $181 \pm 7.7$ ,  $135 \pm 2.6$ , and  $74 \pm 8.3 \mu\text{m}$  for hydrogels prepared using HRP concentrations of 3.9, 7.7, and 15.5  $\text{unit L}^{-1}$ , respectively (Table 2). These macropore sizes after cellulase digestion represent enlargements of 2.1-fold ( $p < 0.0001$ ), 2.6-fold ( $p < 0.0001$ ),

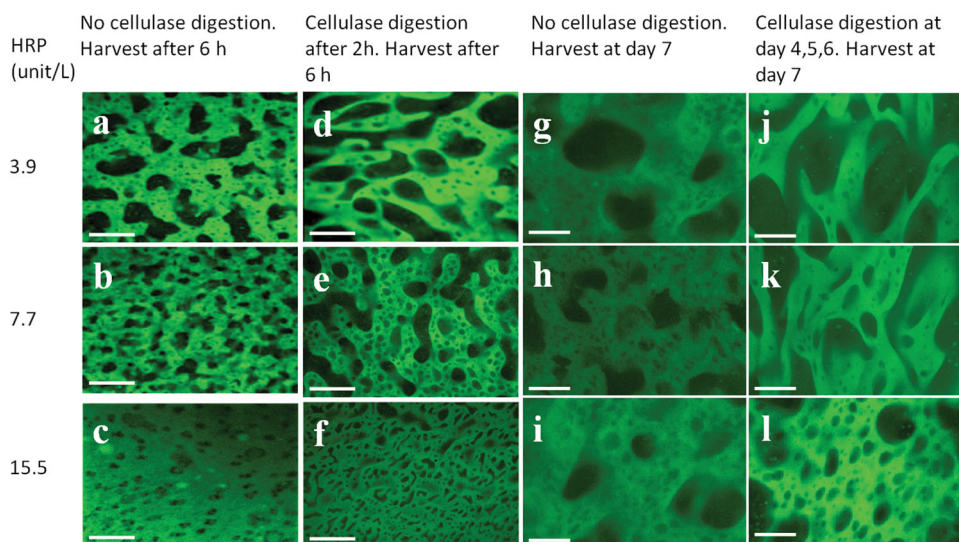


**Figure 8.** a–c) Representative LSCM images of hydrated fluorescently labeled in vivo hydrogels prepared using 3.9, 7.7, and 15.5  $\text{unit L}^{-1}$  HRP, respectively, without cellulase treatment. These hydrogels were harvested 6 h after injection. d–f) Representative LSCM images of hydrated fluorescently labeled in vivo hydrogels prepared using 3.9, 7.7, and 15.5  $\text{unit L}^{-1}$  HRP, respectively, after digestion by cellulase 2 h after hydrogel injection. These hydrogels were harvested 6 h after the initial hydrogel injection. g–i) Representative LSCM images of hydrated fluorescently labeled in vivo hydrogels prepared using 3.9, 7.7, and 15.5  $\text{unit L}^{-1}$  HRP, respectively, without cellulase treatment. These hydrogels were harvested 7 d after injection. j–l) Representative LSCM images of hydrated fluorescently labeled in vivo hydrogels prepared using 3.9, 7.7, and 15.5  $\text{unit L}^{-1}$  HRP, respectively, after digestion by cellulase at day 4, 5, and 6. These hydrogels were harvested 7 d after the initial hydrogel injection. The scale bars represent 200  $\mu\text{m}$ .

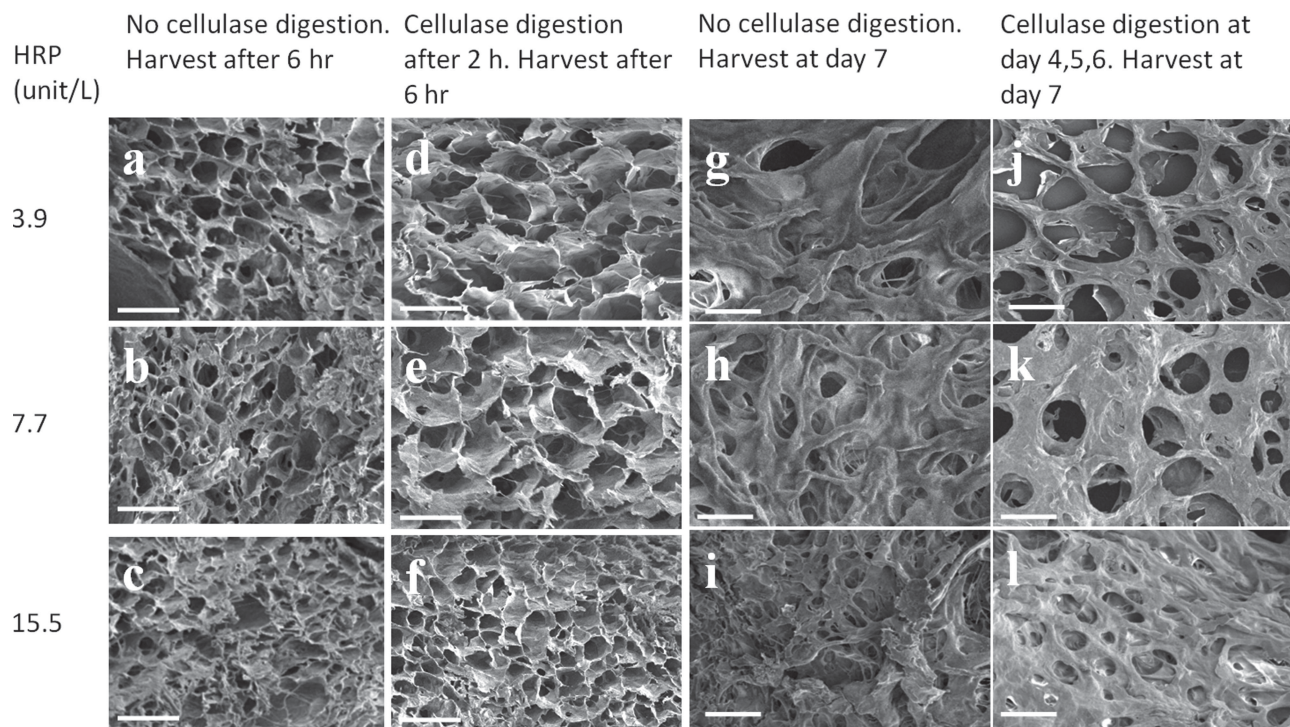


**Figure 9.** a–c) Typical cross-sectional SEM images of lyophilized in vivo hydrogels prepared using 3.9, 7.7, and 15.5 unit L<sup>-1</sup> HRP, respectively, without cellulase treatment. These hydrogels were harvested 6 h after injection. d–f) Typical cross-sectional SEM images of lyophilized in vivo hydrogels prepared using 3.9, 7.7, and 15.5 unit L<sup>-1</sup> HRP, respectively, after cellulase digestion 2 h after hydrogel injection. These hydrogels were harvested 6 h after the initial hydrogel injection. g–i) Typical cross-sectional SEM images of lyophilized in vivo hydrogels prepared using 3.9, 7.7, and 15.5 unit L<sup>-1</sup> HRP, respectively, without cellulase treatment. These hydrogels were harvested 7 d after injection. j–l) Typical cross-sectional SEM images of lyophilized in vivo hydrogels prepared using 3.9, 7.7, and 15.5 unit L<sup>-1</sup> HRP, respectively, after cellulase digestion at day 4, 5, and 6. These hydrogels were harvested 7 d after the initial hydrogel injection. The scale bars represent 200  $\mu\text{m}$ .

and 2.3-fold ( $p < 0.0001$ ), respectively, relative to the corresponding pores in scaffolds without cellulase treatment. In contrast, the average diameter of the smaller pores in the digested

scaffolds was not dependent on HRP concentration ( $p = 0.183$ ), being similar at  $12 \pm 2.7$ ,  $10 \pm 7.4$ , and  $9 \pm 6.2$   $\mu\text{m}$  for 3.9, 7.7, and 15.5 unit L<sup>-1</sup> HRP, respectively. Although micropores in

**Table 2.** Mean macropore and micropore sizes in in vivo Gtn-HPA/CMC-Tyr hydrogels with and without cellulase digestion. Results are shown as mean  $\pm$  standard deviation.

Hydrogels harvested 6 h post-implantation				
HRP concentration [unit L <sup>-1</sup> ]	Mean size of macropores without cellulase digestion [ $\mu\text{m}$ ]	Mean size of micropores without cellulase digestion [ $\mu\text{m}$ ]	Mean size of macropores with cellulase digestion [ $\mu\text{m}$ ]	Mean size of micropores with cellulase digestion [ $\mu\text{m}$ ]
3.9	$87 \pm 2.1$	$19 \pm 3.4$	$181 \pm 7.7^{\text{a}}$	$12 \pm 2.7^{\text{a}}$
7.7	$51 \pm 5.2$	$11 \pm 7.2$	$135 \pm 2.6^{\text{a}}$	$10 \pm 7.4$
15.5	$32 \pm 1.3$	$9 \pm 8.2$	$74 \pm 8.3^{\text{a}}$	$9 \pm 6.2$
Hydrogels harvested 7 d post-implantation				
HRP concentration (unit L <sup>-1</sup> )	Mean size of macropores without cellulase digestion [ $\mu\text{m}$ ]	Mean size of micropores without cellulase digestion [ $\mu\text{m}$ ]	Mean size of macropores with cellulase digestion at days 4, 5, and 6 [ $\mu\text{m}$ ]	Mean size of micropores with cellulase digestion at days 4, 5, and 6 [ $\mu\text{m}$ ]
3.9	$123 \pm 0.9$	$36 \pm 0.4$	$236 \pm 3.6^{\text{a}}$	$63 \pm 6.3^{\text{a}}$
7.7	$81 \pm 2.5$	$27 \pm 5.2$	$177 \pm 8.6^{\text{a}}$	$47 \pm 7.7^{\text{a}}$
15.5	$48 \pm 1.0$	$19 \pm 0.2$	$108 \pm 6.3^{\text{a}}$	$31 \pm 8.1^{\text{a}}$

<sup>a</sup>) At the same HRP concentration and for hydrogels harvested at the same time, the difference between the mean pore size before cellulase digestion and the mean pore size after cellulase digestion is statistically significant at  $p < 0.01$ .

the 3.9 unit L<sup>-1</sup> HRP hydrogels were reduced in size after cellulase treatment ( $p < 0.0001$ ), cellulase digestion had no effect on micropore dimensions in scaffolds prepared using 7.7 and 15.5 unit L<sup>-1</sup> HRP ( $p = 0.630$  and  $p = 0.716$ , respectively). This reflects the relative inaccessibility and lower interconnectivity of the smaller pores for cellulase diffusion, so that the main effect of cellulase treatment was enlargement of the scaffold macropores. As larger pores enhance mass transfer and are preferred during the later stages of tissue regeneration for ECM deposition, an improvement in culture performance and tissue engineering outcomes can be expected after *in situ* cellulase digestion of implanted hydrogels. Whereas the gelatin component of the Gtn-HPA/CMC-Tyr hydrogels is already biodegradable and capable of being adsorbed gradually within the body, directed application of cellulase enzyme allows control to be exercised over the rate of degradation of the cellulose (CMC) component of the polymer matrix.

Depending on the rate of tissue formation *in vivo*, multiple applications of cellulase may be used to further enlarge the hydrogel pores as more space is required in the scaffold. To test this, we studied the effect of introducing cellulase at later time points (cellulase was introduced at days 4, 5, and 6). Figure 8j–l shows typical LSCM images of cross-sections of hydrated hydrogel implants after multiple *in vivo* cellulase treatments. Figure 9j–l shows the corresponding SEM images of the cellulase-treated hydrogels after lyophilization. Table 2 summarizes the pore sizes of *in vivo* hydrogels obtained with or without cellulase digestion. As expected, for each HRP concentration, the mean diameters of the macropores in hydrogels with multiple cellulase treatments were larger than those in hydrogels treated with a single application of cellulase. Interestingly, the mean diameters of the micropores in hydrogels with multiple cellulase treatments were also larger than those in hydrogels with a single-cellulase treatment at the corresponding HRP concentration. This suggests that cellulase can penetrate the micropores if multiple cellulase treatments are given, as larger macropores provide better accessibility for cellulase diffusion into the micropores, thereby allowing the micropores to open up during subsequent cellulase treatment. In addition, the longer implantation time (7 d) also allowed *in vivo* proteases to penetrate and degrade the hydrogels to open up the pores. Consistent with the LSCM results in Figure 8g–l, the SEM images in Figure 9g–l revealed that hydrogels harvested after 7 d were highly porous with interconnected pores. The hydrogel scaffolds harvested after 7 d (Figure 9g–l) appeared to be more collapsed compared to those harvested after 6 h (Figure 9a–f), which is likely due to the reduced mechanical strength caused by cellulase digestion and protease degradation. It is expected that the reduction in mechanical strength associated with scaffold degradation allows new tissue to easily infiltrate the scaffold.

#### 4. Conclusion

The pore structure of an injectable hydrogel scaffold was modified post-implantation in this proof-of-concept work. Using the prepared hydrogel, the properties of the scaffold were tuned *in vivo* by simply injecting a digestive enzyme into the implantation site. In untreated scaffolds, average macropore sizes *in vivo*

ranged from 32 to 87  $\mu\text{m}$  depending on the conditions applied for polymer cross-linking. After tuning of the pore structure using a single cellulase injection, macropore sizes were increased to 74–181  $\mu\text{m}$ , while multiple cellulase injections produced macropore sizes *in vivo* of 108–236  $\mu\text{m}$ . The hydrogel system developed is biodegradable, biocompatible, and suitable for cell culture and tissue engineering applications. The mechanical properties of the biomaterial are similar to those of soft tissues and organs; an additional advantage is that the gelation rate and mechanical properties of the hydrogel can be tuned independently. Using the approach and methods described here, the pore size and porosity of scaffolds can be tailored *in situ* after implantation to match the growth rate of the tissue being regenerated and in response to the recovery conditions of the patient. The system is therefore ideal for personalized tissue engineering.

#### Supporting Information

Supporting Information is available from the Wiley Online Library or from the author.

#### Acknowledgements

T.T.Y.T. and P.P.Y.C. contributed equally to this work. Funding was provided by Australian Research Council (ARC) Discovery Project Grants DP120102570 and DP120100583, and by the Singapore Ministry of Education AcRF Tier 2 ARC16/11. This work was performed in part at the Melbourne Centre for Nanofabrication (MCN) in the Victorian Node of the Australian National Fabrication Facility (ANFF), an initiative funded jointly by the Commonwealth of Australia and the Victorian Government. PC acknowledges the MCN Technology Fellowship and RMIT Senior Research Fellowship that supported this work. The authors acknowledge Douglas Mair and Manoj Sridhar from the Melbourne Centre of Nanofabrication for assistance with the LSCM and SEM imaging.

Received: July 24, 2013

Published online: October 22, 2013

- [1] F. J. O'Brien, B. A. Harley, I. V. Yannas, L. J. Gibson, *Biomaterials* **2005**, *26*, 433.
- [2] S. H. Oh, I. K. Park, J. M. Kim, J. H. Lee, *Biomaterials* **2007**, *28*, 1664.
- [3] D. Huttmacher, T. Woodfield, P. Dalton, J. Lewis, *Tissue Engineering* (Ed: C. Van Blitterswijk), Academic Press, Canada **2008**, Ch. 14.
- [4] S.-M. Lien, L.-Y. Ko, T.-J. Huang, *Acta Biomater.* **2009**, *5*, 670.
- [5] S. Yang, K.-F. Leong, Z. Du, C.-K. Chua, *Tissue Eng.* **2001**, *7*, 679.
- [6] J. Zeltinger, J. K. Sherwood, D. A. Graham, R. Müller, L. G. Griffith, *Tissue Eng.* **2001**, *7*, 557.
- [7] Q. Liu, E. L. Hedberg, Z. Liu, R. Bahulekar, R. K. Meszlenyi, A. G. Mikos, *Biomaterials* **2000**, *21*, 2163.
- [8] S. J. Bryant, J. L. Cuy, K. D. Hauch, B. D. Ratner, *Biomaterials* **2007**, *28*, 2978.
- [9] K. E. Yarasheski, J. J. Zachwieja, D. M. Bier, *Am. J. Physiol. Endocrinol. Metabol.* **1993**, *265*, E210.
- [10] M. Golden, J. C. Waterlow, D. Picou, *Am. J. Clin. Nutr.* **1977**, *30*, 1345.

- [11] A. Barbero, S. Grogan, D. Schäfer, M. Heberer, P. Mainil-Varlet, I. Martin, *Osteoarthritis Cartilage* **2004**, *12*, 476.
- [12] M. Kurisawa, F. Lee, L.-S. Wang, J. E. Chung, *J. Mater. Chem.* **2010**, *20*, 5371.
- [13] M. C. Gómez-Guillén, B. Giménez, M. E. López-Caballero, M. P. Montero, *Food Hydrocolloid* **2011**, *25*, 1813.
- [14] L.-S. Wang, J. E. Chung, P. Pui-Yik Chan, M. Kurisawa, *Biomaterials* **2010**, *31*, 1148.
- [15] M. Hu, M. Kurisawa, R. Deng, C. M. Teo, A. Schumacher, Y. X. Thong, L. Wang, K. M. Schumacher, J. Y. Ying, *Biomaterials* **2009**, *30*, 3523.
- [16] M. Hu, R. Deng, K. M. Schumacher, M. Kurisawa, H. Ye, K. Purnamawati, J. Y. Ying, *Biomaterials* **2010**, *31*, 863.
- [17] L.-S. Wang, J. Boulaire, P. P. Y. Chan, J. E. Chung, M. Kurisawa, *Biomaterials* **2010**, *31*, 8608.
- [18] L.-S. Wang, J. E. Chung, M. Kurisawa, *J. Biomater. Sci. Polym. E.* **2012**, *23*, 1793.
- [19] H.-R. Lee, K. M. Park, Y. K. Joung, K. D. Park, S. H. Do, *J. Controlled Release* **2012**, *159*, 332.
- [20] K. M. Park, K. S. Ko, Y. K. Joung, H. Shin, K. D. Park, *J. Mater. Chem.* **2011**, *21*, 13180.
- [21] W. S. Toh, T. C. Lim, M. Kurisawa, M. Spector, *Biomaterials* **2012**, *33*, 3835.
- [22] T. C. Lim, W. S. Toh, L. S. Wang, M. Kurisawa, M. Spector, *Biomaterials* **2012**, *33*, 3446.
- [23] F. Lee, J. E. Chung, M. Kurisawa, *Soft Matter* **2008**, *4*, 880.
- [24] Y. Shona Pek, M. Kurisawa, S. Gao, J. E. Chung, J. Y. Ying, *Biomaterials* **2009**, *30*, 822.
- [25] K. S. Kim, S. J. Park, J. A. Yang, J. H. Jeon, S. H. Bhang, B. S. Kim, S. K. Hahn, *Acta Biomater.* **2011**, *7*, 666.
- [26] J. A. Burdick, G. D. Prestwich, *Adv. Mater.* **2011**, *23*, H41.
- [27] M. Kurisawa, J. E. Chung, Y. Y. Yang, S. J. Gao, H. Uyama, *Chem. Commun.* **2005**, 4312.
- [28] S. P. Hoo, Q. L. Loh, Z. Yue, J. Fu, T. T. Y. Tan, C. Choong, P. P. Y. Chan, *J. Mater. Chem. B* **2013**, *1*, 3107.
- [29] A. Matalanis, U. Lesmes, E. A. Decker, D. J. McClements, *Food Hydrocolloid* **2010**, *24*, 689.
- [30] S. A. Zawko, C. E. Schmidt, *Acta Biomater.* **2010**, *6*, 2415.
- [31] D. L. Elbert, *Acta Biomater.* **2011**, *7*, 31.
- [32] J. Oh, A. D. Rey, *Macromol. Theor. Simul.* **2000**, *9*, 641.
- [33] K. Luo, *Eur. Polym. J.* **2006**, *42*, 1499.
- [34] US FDA, Cellulase enzyme preparation derived from *Trichoderma longibrachiatum*, Code of Federal Regulations, 21CFR184.1250, **2011**. <http://www.accessdata.fda.gov/scripts/cdrh/cfdocs/cfcfr/CFRSearch.cfm?FR=184.125>. (Access July, 2012).
- [35] V. Tolstoguzov, *Food Hydrocolloid* **2003**, *17*, 1.
- [36] Q. F. Dang, J. Q. Yan, J. J. Li, X. J. Cheng, C. S. Liu, X. G. Chen, *Carbohydr. Polym.* **2011**, *83*, 171.
- [37] I. Levental, P. C. Georges, P. A. Janmey, *Soft Matter* **2007**, *3*, 299.
- [38] S. Ghosh, V. Gutierrez, C. Fernández, M. A. Rodríguez-Pérez, J. C. Viana, R. L. Reis, J. F. Mano, *Acta Biomater.* **2008**, *4*, 950.
- [39] W. Otto, in *Epidermal Cells*, Vol. 289 (Ed: K. Turksen), Humana Press, New Jersey **2005**, 251.